

Rigidified Calixarenes Bearing Four Carbamoylmethylphosphineoxide or Carbamoylmethylphosphoryl Functions at the Wide Rim

Arturo Arduini,^[d] Volker Böhmer,^{*[a]} Laetitia Delmau,^[c] Jean-François Desreux,^{*[b]} Jean-François Dozol,^{*[c]} M. Alejandro Garcia Carrera,^[c] Bernard Lambert,^[b] Christian Musigmann,^[a] Andrea Pochini,^[d] Alexander Shivanyuk,^[a] and Franco Ugozzoli^[e]

Abstract: Conformationally rigidified tetraCMPO derivatives have been prepared from calix[4]arene bis(crown ether) **4a** in which adjacent oxygens are bridged at the narrow rim by two diethylene glycol links. Acylation of the tetraamine **4c** with the CMPO-active ester **5b** gave the tetraphosphine oxide **6a**, while the tetraphosphinate **6b** and the tetraphosphonate **6c** were obtained by Arbuzov reaction of tetrabromoacetamido derivative **7** with PhP(OEt)₂ or P(OEt)₃. The extraction ability of these CMPO derivatives was checked for selected lanthanides and actinides and compared with the analogous compounds **1b**, **10b** and **10d** derived from calix[4]arene tetrapentyl ether. All rigidified bis(crown ether) ligands are more effective extractants than their pentyl ether counterparts and require

only 1/10 of the concentration ($c_L = 10^{-4} \text{ M}$) to obtain the same distribution coefficients, while with CMPO itself a 2000-fold concentration is necessary. This could be a consequence of a better preorganisation of the ligating functions owing to the rigidity which on the other hand did not change the observed selectivity for americium ($D_{Am}/D_{Eu} = 9-19$) and for light lanthanides over heavy ones. NMR relaxivity titration curves show that the complex of Gd³⁺ with ligand **6a** is highly oligomerised in anhydrous acetonitrile over a large range of ligand:metal concentration ratios. Nuclear magnetic relaxation disper-

sion (NMRD) profiles also showed that large oligomers were formed, and their mean tumbling times were deduced from the Solomon–Bloembergen–Morgan equations. The NMR spectra of dia- and paramagnetic lanthanide complexes with **6a** agreed with the presence of two conformers with an elongated calix[4]arene skeleton in which the distances between opposite methylene groups are different. Contrary to what was observed with ligand **2a**, the addition of nitrate ions does not labilize the metal complexes, presumably because of the rigidification effect of the ether bridges. Single-crystal X-ray structures were obtained for the active ester **5b** and for diphenylphosphorylacetic acid **5a**.

Keywords: actinides • calixarenes • complexation • extraction • lanthanides • NMR spectroscopy

Introduction

Calixarenes are macrocyclic compounds in which several phenolic rings are connected by methylene bridges. The ease of their preparation and chemical modification makes them ideal starting materials for the construction of more elaborate molecules.^[1] The calix[4]arene especially has been frequently used as a molecular platform on which to assemble various ligating groups in order to design cationic,^[2] anionic^[3] or even bifunctional receptors.^[4] Preorganisation of such functional groups at the wide or narrow rim of the calix[4]arene resulted in strong binding, predominantly at the cost of the complexation entropy. For example, calix[4]arene acetamides (e.g., **1a**), acetates (e.g., **1b**) and acetic acids (e.g., **1c**), or analogous compounds with mixed functionalities, are effective and selective receptors for sodium,^[5] calcium,^[6] lanthanides,^[7] actinium,^[8] uranium(vi) and thorium(iv).^[9]

In order to obtain selective extractants for lanthanides and actinides in the separation and decontamination of nuclear waste streams, the calix[4]arene tetraethers **2** have been

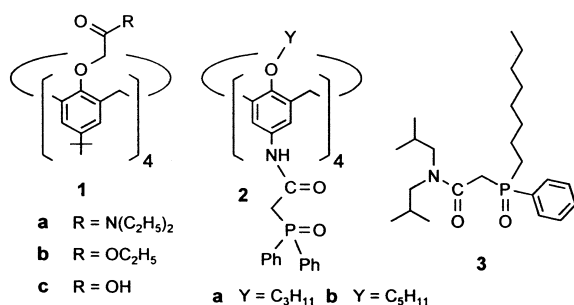
[a] Dr. V. Böhmer, Dr. C. Musigmann, Dr. A. Shivanyuk
Fachbereich Chemie und Pharmazie, Abteilung Lehramt Chemie
Johannes-Gutenberg-Universität Mainz, Duesbergweg 10–14
55099 Mainz (Germany)
Fax: (+49) 6131-3925419
E-mail: vboehmer@mail.uni-mainz.de

[b] Prof. J.-F. Desreux, Dr. B. Lambert
Coordination and Radiochemistry, Sart Tilman-B16,
University of Liège, 4000 Liège (Belgium)
Fax: (+32)4-3663364
E-mail: jf.desreux@ulg.ac.be

[c] Dr. J.-F. Dozol, Dr. L. Delmau, M. A. Garcia Carrera
CEA Cadarache/DES/SEP/LPTE/
13108 Saint Paul Lez Durance Cedex (France)

[d] Prof. A. Arduini, Prof. A. Pochini
Dipartimento di Chimica Organica ed Industriale
Università di Parma, Viale delle Scienze
43100, Parma (Italy)

[e] Prof. F. Ugozzoli
Dipartimento di Chimica Generale e Inorganica
Chimica Fisica e Chimica Analitica, Università di Parma
Viale delle Scienze, 43100, Parma (Italy)



prepared in which four CMPO-like (CMPO = carbamoylmethylphosphineoxide or carbamoylmethylphosphoryl) functions are attached to the wide rim.^[10, 11] In fact, compounds **2** are considerably more effective as extractants for the lanthanides and actinides than CMPO **3**^[12] itself, which is used in the TRUEX process.^[13] Higher extraction values are reached with concentrations of 1/100 or less under various conditions. Furthermore, the wide-rim CMPO calixarenes **2** exhibit a remarkable size selectivity within the series of lanthanide cations.^[14] This selectivity is not observed in calix[4]arenes with four CMPO groups attached to the narrow rim,^[15] although these compounds are still much more efficient than CMPO.

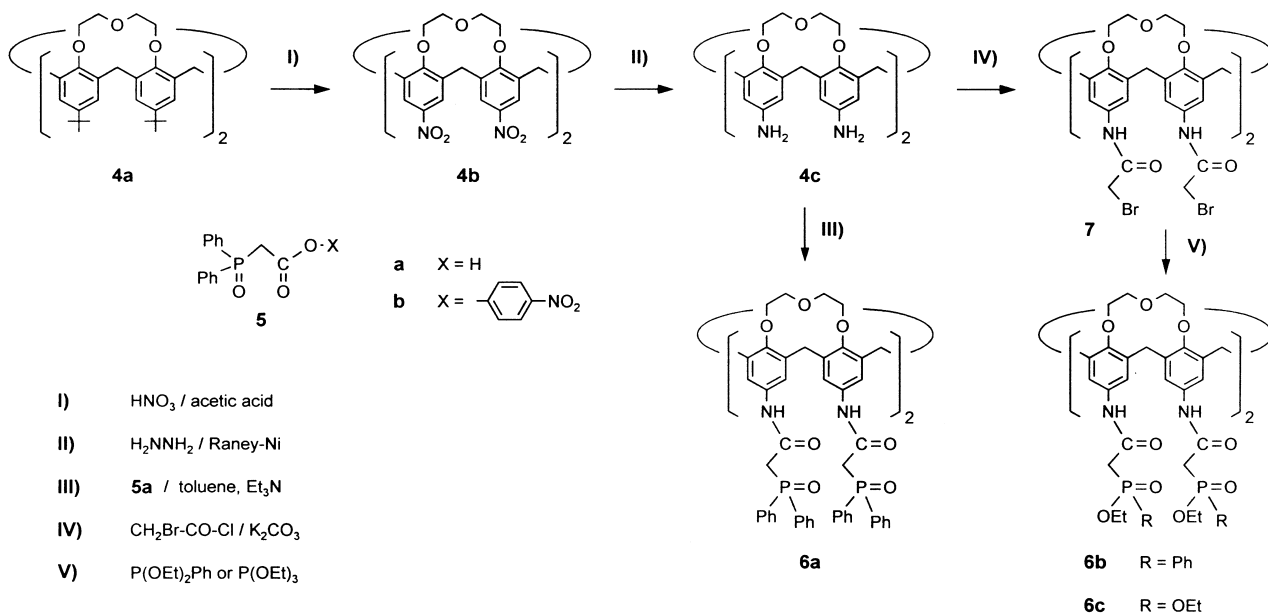
Thus the combination of four ligating functions of the CMPO type is not the only factor that determines the complexation properties. Evidently their mutual orientation and the flexibility of their linkage also has an important influence. It can be assumed that an appropriate balance between rigidity and flexibility of the basic skeleton may also be crucial for an effective coordination.^[16] We recently showed that replacement of alkoxy groups, which cannot pass the annulus (e.g., propyl), with methoxy groups significantly changes the extraction properties of **2**. Although not understood in detail, this must be ascribed to differences in the conformational mobility of the molecules.^[17] In the present

paper we report the synthesis of several conformationally rigidified calixarene tetraCMPO derivatives in which the oxygens in the 1,2- and 3,4-positions are connected by two diethylene glycol links. As shown by an X-ray structure, this leads to a nearly regular cone conformation of the calix[4]-arene skeleton.^[18]

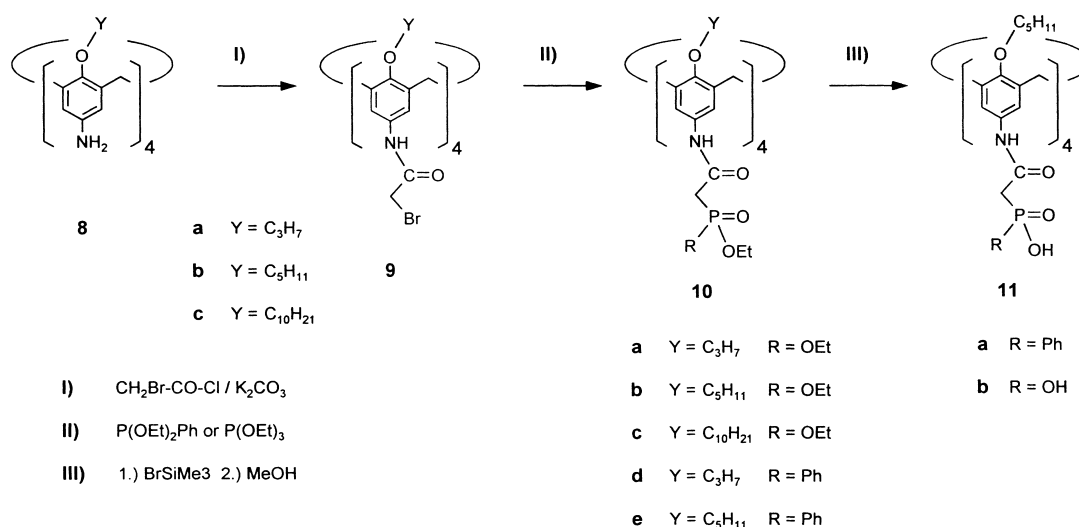
Results and Discussion

Synthesis: The rigidified ligands **6** were prepared as outlined in Scheme 1 by starting with the *tert*-butylcalix[4]bis(crown ether) **4a**.^[18] Reaction of **4a** with fuming HNO₃ in boiling acetic acid gave the tetranitro derivative **4b** (42% yield), which directly precipitated from the reaction mixture in an analytically pure form. This *ipso*-nitration gave better (more reproducible) results than the nitration of the corresponding calix[4]bis(crown ether) with free *p*-positions.^[19] The catalytic reduction (Raney Ni) of the nitro groups with hydrazine in ethanol afforded the tetraamine **4c** in 70% yield, which upon acylation with the active ester **5** (toluene, Et₃N, RT) led to the tetraphosphinoyl **6a** in 62% yield as described for less rigid wide-rim CMPO calixarenes. On the other hand, Schotten-Baumann acylation of **4c** with bromoacetylchloride (K₂CO₃, EtOAc/H₂O) readily gave the tetrabromoacetamide **7**, which was converted into the tetraphosphinate **6b** and the tetraphosphonate **6c** by Arbuzov reaction with P(OEt)₂Ph or P(OEt)₃, respectively. Conformationally mobile calix[4]arene tetraphosphonates **10a–c** and tetraphosphinates **10d,e** were prepared analogously for comparison. Their structure and composition were proved by NMR spectroscopy, mass spectrometry and elemental analysis. For two examples (**10b,e**) it was demonstrated that the corresponding acids **11a,b** are obtainable by reaction with SiMe₃Br followed by methanolysis (Scheme 2).

The ¹H NMR spectrum of compound **6a** measured in [D₆]DMSO shows one singlet for the amide protons, two



Scheme 1.



Scheme 2.

meta-coupled doublets for the protons of the calixarene aryl rings, two pairs of doublets for the methylene bridges and one doublet for the methylene protons of the CMPO fragments. This pattern is entirely consistent with the expected C_{2v} -symmetrical structure. Surprisingly, the ^1H NMR spectrum of **6a** measured in CDCl_3 was broad and featureless, most probably because of association through hydrogen bonds. The self-association of **6a** can be attributed to its rigid structure, since the nonbridged tetraCMPO calixarenes **2** exhibit sharp and well-resolved spectra both in CDCl_3 and in $[\text{D}_6]\text{DMSO}$. Due to the pinching of the cone conformation,^[20] the two opposite CMPO moieties of **2** can form intramolecular hydrogen bonds in nonpolar CDCl_3 ,^[21] while in the case of the bridged compound **6a** the cone conformation cannot be pinched and therefore the CMPO arms must form intermolecular hydrogen bonds; this causes the self-association. It is important to note that the ^1H NMR spectra of compounds **6b** and **6c** are sharp, both in CDCl_3 and in $[\text{D}_6]\text{DMSO}$. This could be explained by the formation of intramolecular hydrogen bonds $\text{N-H}\cdots\text{O}=\text{P}$ in the case of the sterically less-hindered phosphonate and phosphinate fragments.

The 400 MHz ^1H NMR spectrum of tetraphosphinate **6b** measured in $[\text{D}_6]\text{DMSO}$ contains three singlets for the protons of amide groups and three signals for the aromatic protons of the calixarene in the ratio 1:2:1, while the rest of the spectrum is rather complicated. This can be explained by the presence of four chiral phosphorus atoms in the tetraphosphinate **6b**. As a consequence, diastereomers are possible (five in this special case), which makes the ^1H NMR spectrum more complicated.

The chirality of the phosphorus atoms results in two singlets for the protons of the calixarene aryl rings, along with one broadened singlet for the amide protons in the ^1H NMR spectrum (CDCl_3 , 400 MHz) of the more symmetrical tetraphosphinates **10d,e**. However, in the case of corresponding tetraacid **11a**, only one sharp signal was observed for the aromatic protons of the calixarene skeleton in CD_3OD , most probably due to the fast proton exchange ($\text{HO}-\text{P}=\text{O} \rightarrow \text{O}=\text{P}-\text{OH}$), which makes the phosphorus achiral on the NMR timescale.

Extraction studies: The extraction ability of **6a** was preliminarily established for some lanthanides in the chloroform/(4 M NaNO_3 /0.01 M HNO_3) system. This immediately showed that **6a** is much more efficient than **2b**, which was used for comparison. As shown in Table 1, essentially the same distribution coefficients D were obtained for $c(\mathbf{6a}) = 10^{-4}\text{M}$ as for $c(\mathbf{2b}) = 10^{-3}\text{M}$. The extremely low concentration of **6a** is best illustrated by the fact that a more than 2000-fold concentration of CMPO is required to reach D values of nearly the same magnitude.

Table 1. Distribution coefficients D for the extraction of lanthanides from an aqueous phase ($c(\text{Ln}) = 10^{-6}\text{M}$ in 4 M NaNO_3 ; 0.01 M HNO_3) by CMPO **3** and CMPO-substituted calixarenes in chloroform.

	Pm	Eu	Gd	Tb	Ho	Er
$c(\mathbf{3}) = 0.2\text{M}$	0.44	0.62	0.5	–	0.51	0.34
$c(\mathbf{2b}) = 10^{-3}\text{M}$	15.2	5.2	2.4	0.8	0.4	0.22
$c(\mathbf{6a}) = 10^{-4}\text{M}$	14.6	4.7	2.7	1.5		

This high extraction efficiency for compounds **6** makes comparative studies with similar ligands under standard conditions difficult, since either the distribution coefficients are in an extremely high (and less reliable) region or the ligand concentration must be so low that it is no longer in large excess with respect to the extracted cations.

Since many studies on CMPO-substituted calixarenes have been done with *o*-nitrophenylhexylether (NPHE), an organic solvent that is also suitable as an organic phase in supported liquid membranes, NPHE was used for all further studies with compounds **6** and **10** with different concentrations of HNO_3 as the aqueous phase.

As usual for ligands of the CMPO type, they are effective in strongly acidic solution. As an example, Figure 1 shows the distribution coefficient of **6b** for various cations as a function of the HNO_3 concentration. A similar maximum around $c(\text{HNO}_3) = 2\text{--}3\text{M}$ is also observed for compounds of type **2**, while it is less pronounced for **6c**, for which the distribution coefficients reach a plateau for the higher concentrations of nitric acid.

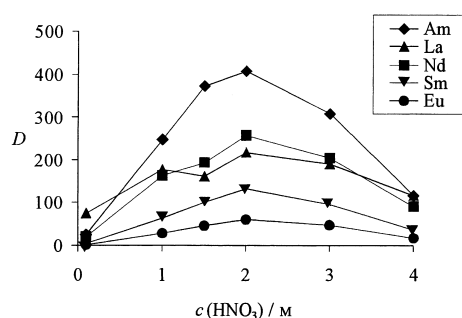


Figure 1. Distribution coefficient D for the extraction of different cations by **6b** in NPHE ($c_L = 10^{-3}$ M) as a function of the concentration of nitric acid.

Figure 2 compares, for the same cations, the distribution coefficients D (at $c(\text{HNO}_3) = 3$ M) of the three rigidified calix[4]arenes **6a–c** with those of **2b** as a standard model. For all cations, D decreases in the order **6a** > **6b** >> **6c**, which is in agreement with the decreasing basicity of the phosphoryl groups. It was previously found that phosphine oxides that display the highest basicity are better extractants than phosphinates, while phosphonates are even less effective.^[22] The standard carbamoylmethylphosphineoxide calix[4]arene **2b** is always a slightly weaker extractant, than the rigid carbamoylmethylphosphinate **6b**.

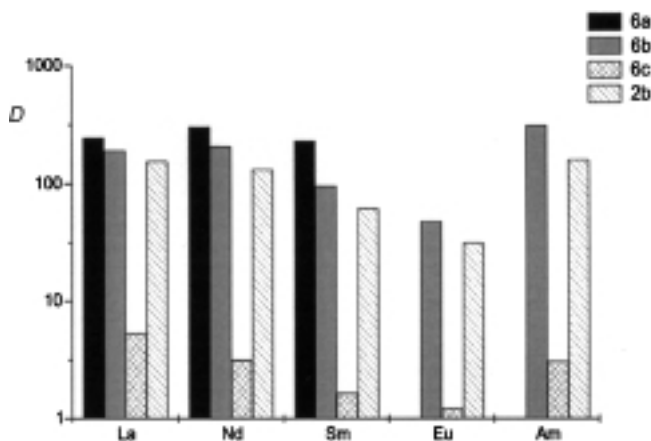


Figure 2. Extraction of different cations from 3 M HNO_3 ($c_L = 10^{-3}$ M) by calixarenes **6a–c** compared with **2b**, in NPHE. For Eu and Am, extremely high values were obtained for the distribution coefficient ($D > 1000$) which are no longer reliable.

Table 2 compares (as an example) the extraction of Eu by the rigidified bis(crown ether) derivatives and by their tetrapentyl ether analogues at various concentrations of nitric acid. The results may be generalised by stating that the rigid compounds are more efficient by a factor of ten than the corresponding “normal” tetraether derivatives. This is true for all the cations studied, which also implies that the selectivities observed for **2** or **10** are kept in the analogous derivative **6**.

In order to study the most efficient extractant **6a** in more detail, a series of extraction experiments were carried out with different (lower) concentrations of this ligand. These results are collected for ^{241}Am and ^{244}Cm in Table 3, in which values for ^{152}Eu are included for comparison. Due to the high

Table 2. Comparison of the rigid bis-crown ether derivatives **6a–c** with the corresponding pentylether derivatives **2b**, **10d** and **10b**. Distribution coefficients of Eu for different concentrations of nitric acid; $c_L = 10^{-3}$ M.

	$c(\text{HNO}_3)$ [M]					
	0.01	0.1	1	2	3	4
2b	0.2	2	30	56	45	29
10d	0.02	0.06	2	4	6	4
10b			< 0.1			
6a	1	93		> 500		
6b	0.04	2	29	61	48	18
6c	0.3	0.3	0.5	1	2	2

Table 3. Distribution coefficients of Am, Cm and Eu for different concentrations of nitric acid and different concentrations of the ligand **6a**.

c_L [M]	cation	$c(\text{HNO}_3)$ [M]					
		0.01	0.1	1	2	3	4
10^{-3}	Am	13	397			> 1000	
	Cm	5			> 100		
	Eu	1.1	93			> 1000	
3×10^{-4}	Am	4	40	87	103	146	116
	Cm	2	32	84	69	90	65
	Eu	0.35	7.1	67	59	68	35
10^{-4}	Am	0.02	1.4	70	36	19	8.9
	Cm	0.02	0.7	21	22	12	9.0
	Eu	0	0.12	3.7	4.1	2.7	1.5

extraction efficiency of this ligand, the distribution coefficients determined for the lowest c_L seem to be more reliable. Here, the separation factor $D_{\text{Am}}/D_{\text{Eu}}$ decreases from 19 at $c(\text{HNO}_3) = 1$ M to about 6 for $c(\text{HNO}_3) = 4$ M, which roughly corresponds to the separation factors found for **2b** when chloroform is used as the organic phase.

Finally, the results of competitive extractions of selected lanthanides and americium are shown in Figure 3 for various concentrations of nitric acid. Under these conditions ($c_L = 10^{-4}$ M), a very strong extraction of lanthanum occurs and (in

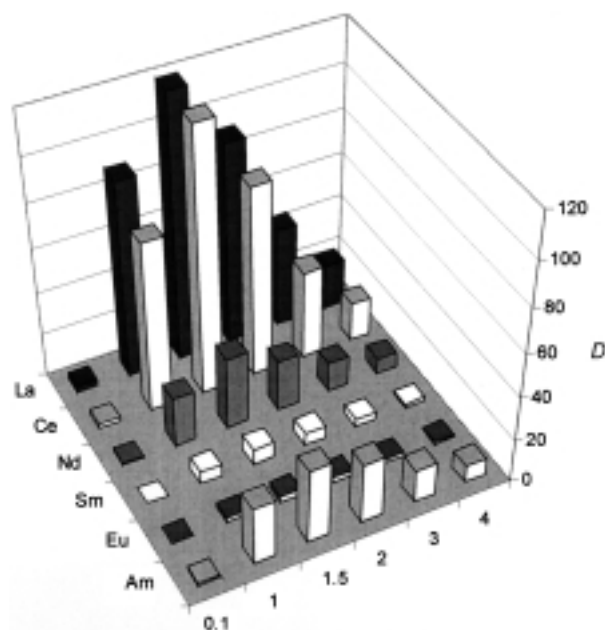


Figure 3. Extraction of light lanthanides [$c(\text{Ln}) = 10^{-6}$ M] and americium (at trace level) by **6a** in NPHE ($c_L = 10^{-4}$ M).

contrast to **2b**, which is not shown) also of cerium. The distribution coefficients (showing a maximum for $c(\text{HNO}_3) = 1.5\text{M}$) decrease with increasing atomic number and, already, for europium they are lower than those for americium (see also Table 3), as observed earlier for **2b** in extractions with chloroform. Evidently this selectivity is levelled at higher ligand concentrations (see Figure 3) by the excellent extraction efficiency of **6a**.

It should be noted that the apparent distribution coefficients strongly decrease if the concentration of the lanthanides is increased by a factor of ten. This is most likely due to the competition between cations for the relatively lower capacity of the extractant. However, the selectivity is approximately maintained and would still be sufficient to separate Am from the preferentially extracted La and Ce and the poorly extracted Eu and Sm. On the other hand, for cation concentrations of $c(\text{Ln}) = 10^{-5}\text{M}$, the distribution coefficients are relatively independent of $c(\text{HNO}_3)$ in the range of 1–4M, while they show a strong decrease for higher acid concentrations (Figure 3) for $c(\text{Ln}) = 10^{-6}\text{M}$. At these low concentrations of lanthanides the competitive extraction of nitric acid is probably not negligible.

NMR spectroscopic studies: NMR spectroscopy has proved extremely valuable for unravelling the solution structures of paramagnetic lanthanide chelates with a variety of ligands.^[23] Of particular relevance are the very large NMR shifts induced by Yb^{3+} and the significant reduction of the relaxation times of the solvent brought about by Gd^{3+} . The former are directly related to the solution conformation of the complexes, while the latter yields information on their solution dynamics. A detailed study of the conformation and the dynamic behaviour of the lanthanide complexes with various calix[4]arenes in anhydrous acetonitrile was reported in an earlier paper.^[24] It was shown that the encapsulation of Gd^{3+} is accompanied by an increase of the T_1 relaxation time of the solvent, because solvent molecules are removed from the first coordination sphere of the metal ion and are allowed to relax independently of the paramagnetic centres. The relaxivity $1/T_1$ expressed in s^{-1} per mm of metal ion therefore decreases until a plateau is reached when the metal complex is fully formed. This behaviour is presented in Figure 4 in the case of tetraamide calix[4]arene **1a** dissolved in anhydrous acetonitrile, the measurements were performed at a fixed frequency of 20 MHz.^[24] As shown previously, the relaxation titration curve recorded for tetracarbamoylmethylphosphineoxide calix[4]arene **2a** does not exhibit the expected break at a 1:1 ligand: Gd^{3+} ratio. Instead of decreasing, the relaxivity reaches a maximum that is followed by a slow decrease until a plateau appears for a threefold excess of ligand. This unusual behaviour has been ascribed to the formation of oligomers.^[24] Indeed, the relaxivity of a solution is dominated by the smallest of three correlation times, namely τ_m , the solvent mean residence time, τ_r , the mean rotation time of the Gd^{3+} complex, and τ_e , the electronic relaxation time of the metal ion. Small complexes rapidly rotate, and the relaxivity of their solutions remains relatively small and essentially dependent on the τ_r value. In contrast, the relaxivity of solutions of slowly tumbling macromolecules can be very high because the

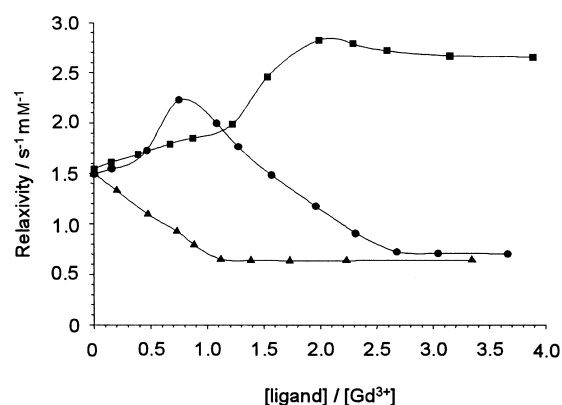


Figure 4. Plots of the observed relaxivity (longitudinal relaxation rates $1/T_1$ in $\text{s}^{-1}\text{mm}^{-1}$ at 25°C and 20 MHz) of anhydrous acetonitrile solutions vs. the ligand/ Gd^{3+} concentration ratio. (\blacktriangle : ligand **1a**; \bullet : ligand **2a**; \blacksquare : ligand **6a**).

electronic relaxation time τ_e and the exchange time τ_m become the dominant factors. As τ_e is frequency dependent, a relaxivity maximum appears at about 20 MHz,^[23, 25] that is, under the conditions already used for the experiments presented in Figure 4. It therefore seems that the increase in relaxivity owing to the slow rotation of oligomeric $\text{Gd}^{3+} \cdot \mathbf{2a}$ species overcomes the relaxivity decrease caused by the release of solvent molecules. At high ligand:metal ratios, the relaxivity of the solutions of the Gd^{3+} complexes with **1a** and **2a** are comparable, and essentially monomeric species are assumed to be present in solutions in both cases.^[24] This interpretation agrees with small-angle neutron-scattering studies^[26] of Pr^{3+} complexes with simple carbamoylmethylphosphineoxide ligands and also with a recently reported crystallographic analysis of the dimeric structure $[\text{Eu}_2\mathbf{2a}_2(\text{NO}_3)_{15}] \cdot 2\text{H}_2\text{O}$, in which one of the metal ions is coordinated to two carbamoylphosphineoxide arms belonging to different calixarene units.^[27] As is clearly shown in Figure 4, the relaxivity titration curve of **6a** significantly differs from that of **2a**. A relaxivity maximum is reached for a ligand **6a**: metal ratio of about two and is followed by a plateau at a much higher relaxivity than in the case of calixarenes **2a** and **1a**. It thus seems that the more rigid skeleton of **6a** favours the formation of oligomeric species even in the presence of a large excess of ligand.

This finding is corroborated by the nuclear magnetic relaxation dispersion (NMRD) curves recorded for two $\mathbf{6a}:\text{Gd}^{3+}$ ratios and reproduced in Figure 5. As reported earlier,^[24] the NMRD curves of uncomplexed Gd^{3+} and of its rapidly tumbling complex with ligand **1a** display the expected S shape with an inflection point between 5 and 10 MHz.^[23, 25] The relaxivity of the $\text{Gd}^{3+} \cdot \mathbf{1a}$ species is lower than that of the uncomplexed ion simply because the solvation of the latter by acetonitrile is much higher. By contrast, the marked relaxivity maxima at about 25 MHz in the NMRD curves indicate that the $\text{Gd}^{3+} \cdot \mathbf{2a}$ and $\text{Gd}^{3+} \cdot \mathbf{6a}$ complexes are highly oligomerised, and that especially large assemblies are formed in the latter case. The shape of the NMRD curves is accounted for by the Solomon–Bloembergen–Morgan equations^[23, 25] and depends essentially on the correlation times τ_m , τ_r and τ_e mentioned above. These parameters have been estimated by a

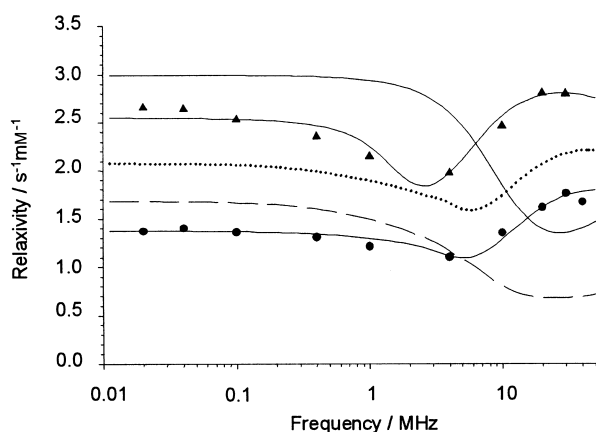


Figure 5. Nuclear magnetic relaxation dispersion curves of anhydrous solutions of uncomplexed Gd^{3+} (solid line), 1:1 mixtures of Gd^{3+} with ligands **1a** (dashed line) and **2a** (dotted line), 1:1 and 1:2 mixtures with ligand **6a** (● and ▲, respectively) at 25 °C in anhydrous acetonitrile. The data presented for free Gd^{3+} , $\text{Gd}^{3+} \cdot \mathbf{1a}$ and $\text{Gd}^{3+} \cdot \mathbf{2a}$ are taken from ref. [25] and the experimental points are excluded for clarity. The lines through the data points result from a least-square treatment of the Solomon–Bloembergen–Morgan equations.

best fit treatment^[28] of the relaxivity data reproduced in Figure 5 by using the only τ_m value reported so far for uncomplexed Gd^{3+} in acetonitrile^[29] ($\tau_m = 200$ ps). The approximate minimum values of τ_r were calculated as 483 and 889 ps for the 1:1 and 1:2 mixtures of Gd^{3+} and ligand **6a**, respectively. These values should be compared with rotational correlation times of 649, 193 and 51 ps for $\text{Gd}^{3+} \cdot \mathbf{2a}$, $\text{Gd}^{3+} \cdot \mathbf{1a}$ and free Gd^{3+} , respectively.^[24] It is noteworthy that high molecular weight (61.8 kD) fifth-generation dendrimers substituted with Gd^{3+} chelates have a τ_r of about 870 ps in water.^[30] One can thus assume that $\text{Gd}^{3+} \cdot \mathbf{6a}$ is highly oligomerised especially since the viscosity of acetonitrile is lower than that of water. It has been suggested that the lanthanide complexes with simple linear carbamoylmethylphosphineoxide ligands form long polymeric chains (length from 150–500 Å) in benzene, and a similar process is probably taking place in the case of the calixarenes **2a** and **6a**.

These studies do not yet permit firm conclusions to be drawn as to why the ether bridges of **6a** favour the formation of oligomers in a large range of ligand:metal ratios, but it is tempting to associate this phenomenon with the very high affinity of **6a** for lanthanides in extraction systems and with the better resistance of $\text{Yb}^{3+} \cdot \mathbf{6a}$ to the competition of nitrate ions and water for the complexation of metal ions

(vide infra). In the present case, a higher stability of the complexes seems to be accompanied by a higher oligomerisation in a wider range of ligand:metal ratios as already reported for linear ligands.^[26] It should probably be emphasised that nuclear magnetic relaxation dispersion appears to be a very interesting, but as yet largely unexplored, area of research in solvent extraction studies. More accurate information will be extracted from the NMRD curves once some of the correlation times have been determined independently.

A detailed study of the solution conformation of the complexes formed between ligand **2a** and anhydrous lanthanide perchlorate salts in acetonitrile has shown that the encapsulation of a lanthanide ion lowers the apparent C_{4v} symmetry of free ligand **2a** to C_{2v} , as evidenced by the observation of two *meta*-coupled NMR peaks for the aromatic protons in the calix and of four doublets for the bridging methylene groups. Twice as many peaks are observed for the calix group in the ^1H spectra of both $\text{La}^{3+} \cdot \mathbf{6a}$ and $\text{Yb}^{3+} \cdot \mathbf{6a}$ (Figure 6) although an analysis of the complete spectra is impossible because of the overlap of numerous peaks. A doubling of the ^{13}C peaks of $\text{La}^{3+} \cdot \mathbf{6a}$ also takes place. In addition, the COSY patterns in the spectrum of $\text{La}^{3+} \cdot \mathbf{6a}$ are in keeping with the presence of eight different protons in the CH_2 bridging groups that are coupled together in pairs. These protons are divided into two groups with peaks of relative areas 1:1 and 3:7 in the case of $\text{La}^{3+} \cdot \mathbf{6a}$ and $\text{Yb}^{3+} \cdot \mathbf{6a}$, respectively. These spectral features are in accord with the coexistence of two conformers in solution. The relative population of the conformers depends on the ionic radius of the metal ion. As no exchange peaks could be found in the EXSY spectra of $\text{La}^{3+} \cdot \mathbf{6a}$ and $\text{Yb}^{3+} \cdot \mathbf{6a}$, one is led to assume that the exchange between the conformers is too slow to be observed at 400 MHz.

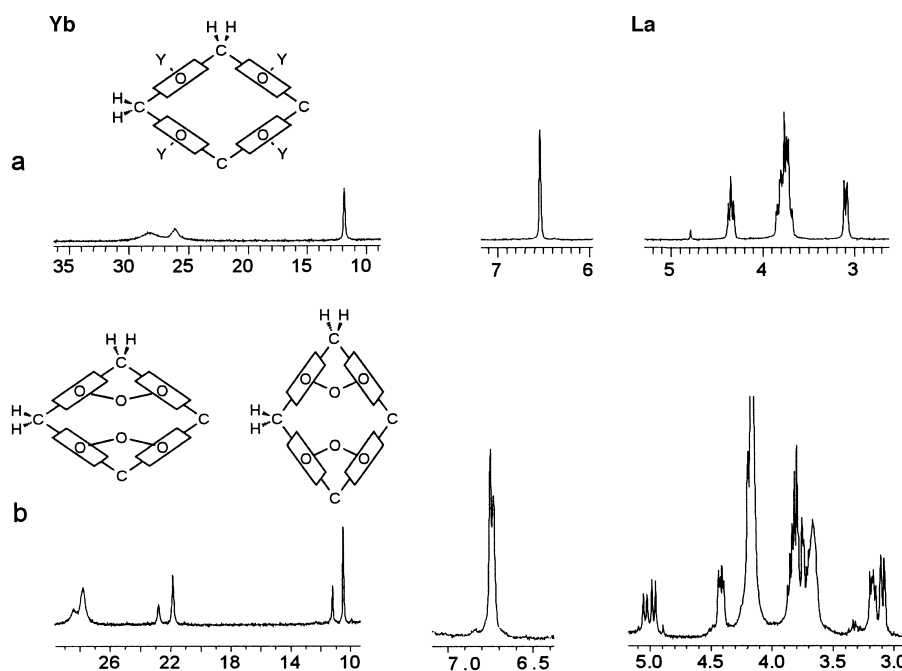


Figure 6. ^1H NMR spectra (details) of the La^{3+} (center and right) and Yb^{3+} complexes (left) with calixarenes **2a** (upper part) and **6a** (lower part). The schematic presentation characterizes the elongated conformation of the calixarene skeleton in the lanthanide complexes with ligand **2a** and shows the two possibilities for **6a**.

The origin of the twofold symmetry of the complexes with **2a** could not be established with certainty, but is probably due to an elongation of the calix skeleton brought about by the steric requirements of the coordination sphere of the lanthanide ions.^[24] Under this assumption, the lanthanide complexes of **6a** should adopt two rigid conformations which differ in the direction of the elongation that takes place either towards the ether bridges or in the perpendicular direction, as illustrated in Figure 6. In each conformer, there are two magnetically non-equivalent environments for the aromatic protons in the calix unit and four different locations for the protons in the bridging methylene groups; this explains the number of resonances found in the NMR spectra. One conformer of the Yb³⁺ complex is less abundant than the other, presumably because of the rigidification effect of the ether bridges. A semi-quantitative analysis of the solution conformation of Yb³⁺·**2a** based on the dipolar equations was possible after full assignment of all the ¹H peaks. Such an analysis is not feasible in the case of **6a** because of the poor resolution of parts of the spectrum.

All the above measurements were performed with anhydrous solutions. Nitrate ions and/or water can be added in order to more closely resemble the experimental conditions used in solvent extraction processes. The addition of tetramethylammonium nitrate to an anhydrous solution of Yb³⁺·**2a** (1:1 ligand:metal ratio) significantly modifies the ¹H NMR spectrum: all resonances become broad and cover a much smaller shift range (ca. 10 ppm instead of 60 ppm). The NO₃⁻ ion is thus able to compete with ligand **2a** and to coordinate directly to Yb³⁺. The resulting complexes are much less rigid, which explains the broad poorly shifted peaks. Adding an excess of tetramethylammonium nitrate to a 1:1 mixture of Yb³⁺ and ligand **6a** also leads to a broadening of the resonances, but the induced paramagnetic shifts are barely altered. Ligand **6a** thus forms more stable lanthanide complexes than calixarene **2a** and its higher extraction efficiency is not surprising. Similar results are obtained after addition of water. Presumably, the two ether bridges help to better define a cavity for the coordination of the metal ions.

Single-crystal X-ray analysis: Single crystals could be obtained for the diphenylphosphoryl acetic acid **5a** from methylene chloride/ethanol and for the active ester **5b**, by slow recrystallization of the crude *p*-nitrophenol-containing material from CH₂Cl₂/hexane.

Two crystallographically independent molecules are found for the acid **5a** in the crystalline state. They are arranged around a centre of symmetry to form cyclic tetramers (Figure 7 top) by intermolecular C(O)O–H···O=P hydrogen bonds. The crystallographic analysis revealed that **5b** forms a crystalline 1:1 complex with *p*-nitrophenol, which is bound to the phosphoryl group by a strong O–H···O=P hydrogen bond (Figure 7 bottom). This structure provides an explanation for

Table 4. Summary of crystal data,^[a] data collection, and structure solution and refinement.

	5a	5b
formula	C ₁₄ H ₁₃ O ₃ P	C ₂₀ H ₁₆ NO ₃ P · C ₆ H ₅ NO ₃
<i>M</i> _w	260.23	520.43
crystal system	triclinic	triclinic
space group	P-1	P-1
<i>T</i> [K]	295	295
<i>a</i> [Å]	12.353(3)	13.127(3)
<i>b</i> [Å]	12.846(2)	11.315(2)
<i>c</i> [Å]	9.501(2)	9.222(2)
α [°]	111.38(2)	103.82(2)
β [°]	105.73(2)	73.75(2)
γ [°]	99.44(2)	108.39(2)
<i>V</i> [Å ³]	1291.9(6)	1230.7(5)
<i>Z</i>	4	2
ρ_{calcd} [g cm ⁻³]	1.338	1.404
<i>F</i> (000)	544	540
μ [cm ⁻¹]	18.76	14.64
diffractometer	Siemens AED	Enraf-Nonius CAD4
scan type	$\theta/2\theta$	$\theta/2\theta$
scan speed [° min ⁻¹]	3	0.053
scan width [°]	$[\theta - 0.6], [\theta + 0.6 + \Delta\lambda\lambda^{-1}\text{tg}\theta]$	$[\theta - 0.6], [\theta + 0.6 + \Delta\lambda\lambda^{-1}\text{tg}\theta]$
radiation	Cu _{Kα} (1.54178 Å)	Cu _{Kα} (1.54178 Å)
2θ range [°]	6–140	6–140
index range	$\pm h, \pm k, +l$	$\pm h, \pm k, +l$
reflns. measured	4875	4671
unique reflns. [$I \geq 2\sigma(I)$]	4173	4046
parameters	429	418
max Δ/σ on last cycle	0.07	0.07
$R = \sum \Delta F / \sum F_o $	0.057	0.051
$wR = \sum w^{1/2} \Delta F / \sum w^{1/2} F_o $	0.057	0.051
GOF = $[\sum w^{1/2} \Delta F ^2 / (n - p)]^{1/2}$ ^[b]	0.82	0.72

[a] Unit cell parameters were obtained by least-squares analysis of the setting angles of 30 carefully centered reflections found in a random search on the reciprocal space. [b] *n* = number of observed reflections, *p* = number of parameters.

why **5b** is difficult to purify by recrystallization, since the 1:1 complex crystallizes much more readily than the pure active ester **5b**. We therefore have started to use the 1:1 complex in preparative acylations instead of the pure active ester **5b**.

Bond lengths and bond angles in both structures (Table 5 contains some selected values) are in the expected range.

Conclusion

The fixation of the calix[4]arene skeleton in a nearly ideal fourfold symmetry by two short crown ether bridges in compounds **6** leads to a strong increase of their extraction ability relative to the analogous compounds **2** or **10**. A similar effect was observed for the complexation of amino acids and ammonium cations by peptidocalix[4]arenes substituted at the wide rim by four L-alanyl residues.^[31] It may be explained in both cases by intramolecular (cross cavity) hydrogen bonds between NH and O=C or O=P functions; this leads to a “closed cavity” and competes with the complexation of the guest. On the other hand, the more pronounced preorganisation of the CMPO functions in ligands **6** does not change the extraction selectivity significantly, as one might expect for a size selective binding of cations in a 1:1 complex. It was shown earlier, however, that CMPO-like substituents on the wide rim of calix[4]arenes are involved in oligomeric structures.^[24] The relaxivity data reported here clearly show that the lanthanide complexes with the bridged ligand form partic-

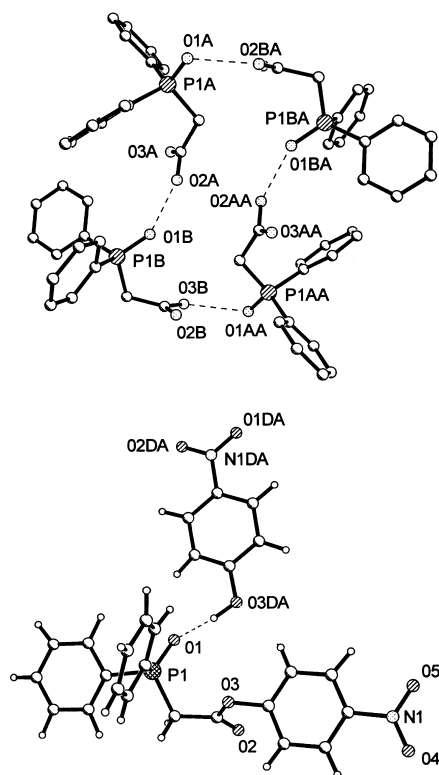


Figure 7. Top: Molecular conformation of **5a** and arrangement of hydrogen bonded tetramers around a center of symmetry. [Hydrogen-bond parameters of the two symmetry-independent hydrogen bonds: Donor–H...Acceptor O2A–H...O1B 172(6)°, O2A–H 1.07(6) Å, O2A...O1B 2.573(3) Å, H...O1B 1.51(6) Å; O3B–H...O1AA 160(4)°, O3B–H 0.96(4) Å, O3B...O1AA 2.572(3) Å, H...O1AA 1.65(4) Å]. Bottom: Molecular conformation and hydrogen bonding in **5b**·*p*-nitrophenol. [Hydrogen bond parameters: Donor–H...Acceptor O3DA–H...O1 172(4)°, O3DA–H 0.88(3) Å, O3DA...O1 2.642(3) Å, H...O1 1.77(4) Å].

Table 5. Selected bond lengths [Å] and angles [°] for compounds **5a** and **5b**.

	5a (molecule A)	5a (molecule B)	5b
P1–O1	1.500(3)	1.497(2)	1.494(3)
P1–C1A	1.794(4)	1.783(5)	1.797(4)
P1–C1B	1.796(4)	1.792(4)	1.794(3)
P1–C1	1.807(5)	1.809(4)	1.807(4)
C1–C2	1.506(5)	1.504(5)	1.488(4)
C2–O2	1.190(6)	1.212(5)	1.191(4)
C2–O3	1.305(5)	1.320(6)	1.360(3)
O3–C1C			1.399(3)
C1A–P1–C1B	107.2(2)	106.6(2)	106.2(1)
C1–P1–C1B	109.2(2)	105.8(2)	104.9(1)
O1–P1–C1B	112.1(2)	111.5(2)	112.1(1)
O1–P1–C1A	110.7(2)	113.4(2)	108.4(2)
O1–P1–C1	110.6(2)	110.5(2)	112.7(2)
P1–C1–C2	117.1(3)	109.0(3)	115.3(2)
O3–C2–C1	113.3(3)	112.6(3)	111.4(2)
O2–C2–C1	123.5(4)	123.0(4)	125.4(3)
O2–C2–O3	123.1(4)	124.4(4)	123.2(3)
C2–O3–C1			117.4(2)

ularly large oligomers. Competition NMR experiments (nitrate, water) also indicate, that the ether bridges rigidify the geometry of the complexes, and this may contribute to the extraction efficiency of **6a** in comparison with **2**. However, it must be stated, that the exact composition and shape of the

extracted complex is not yet known. Many results indicate that several species may be involved and further experiments are necessary to understand the excellent extraction properties of CMPO calixarenes **2** and especially **6** in detail.

Experimental Section

Synthesis

Reagents and methods: Melting points were determined with a MEL TEMP 2 capillary melting point apparatus and are uncorrected. The routine ^1H and ^{13}C NMR spectra were measured with Bruker AC200 and Bruker AM400 spectrometers. FD mass spectra were recorded with a Finnigan MAT 90 (5kV/10 mA min $^{-1}$).

Tetranitro calixarene 4b: The bis(crown ether) **4a** (1.0 g, 1.27 mmol) was dissolved in glacial acetic acid (25 mL) by heating to about 100 °C. HNO₃ (100%, 3 mL) was added in one portion to this solution. An immediate reaction occurred (caution!) and a colourless precipitate formed within 3–5 min. After 10–20 min of stirring, the precipitate was filtered off, washed with glacial acetic acid (2 × 5 mL) and methanol (5 mL) and dried in vacuo. In order to remove traces of acetic acid, the crude product was treated with hot toluene, and the solvent was evaporated in vacuo. This procedure was repeated three times, after which the slightly yellowish solid product **4b** was dried under vacuum at 60 °C for 2–3 h. Yield 0.4 g, (42%); m.p. 299–300 °C (decomp., no clear melting; ref. [18] m.p. 275 °C); NMR data were as reported in the literature.

Tetraamino calixarene 4c: Hydrazine hydrate (2 mL) was added to a suspension of the tetranitro compound **4b** (0.3 g, 0.4 mmol) and Raney Ni (1 g) in EtOH (30 mL). The mixture was heated at reflux for 6 h with further additions of hydrazine hydrate (2 mL every 2 h). After about 4 h, the material was completely dissolved. The solution was evaporated in vacuo. The residue was dissolved again in EtOH/toluene (1:1, 10 mL) and evaporated; this was repeated three times to remove water and EtOH. Finally the product was precipitated from ethanol/hexane. White solid; yield 0.2 g (80%); ^1H NMR (400 MHz, [D₆]DMSO): δ = 6.21 (brs, 4H; Ar-H), 6.20 (brs, 4H; ArH), 4.68 (d, J = 11.4 Hz, 2H; CH₂), 4.40–3.95 (m, 22H; OCH₂, NH₂, CH₂), 3.55–3.45 (m, 4H; OCH₂), 2.85, 2.78 (2d, J = 11.4 Hz, each 2H; CH₂).

Tetraphosphineoxide 6a: Triethylamine (3 mL) and the active ester **5b** (0.7 g, 1.8 mmol) were dissolved in warm toluene (15 mL) and added to a suspension of the tetraamino **4c** (0.2 g, 0.32 mmol) in dry toluene (15 mL). After about 0.5 min, an oily precipitate was formed. The solution was removed and the precipitate was dissolved in CH₂Cl₂ (5 mL) and both solutions were combined again. The reaction mixture was stirred at RT for 10 h, CH₂Cl₂ (50 mL) was added and the solution was washed with aqueous NaOH (1M) until the aqueous layer was colourless (3 × 50 mL) and then with water (2 × 50 mL). After evaporation in vacuo, water was removed azeotropically using a mixture of EtOH and toluene. The crystalline product thus obtained was dissolved in CH₂Cl₂ and reprecipitated with hexane (twice). Yield 0.3 g (62%); yellowish solid; m.p. 211–213 °C; ^1H NMR (400 MHz, [D₆]DMSO): δ = 9.77 (s, 4H; NH), 7.85–7.75 (m, 16H; ArH), 7.60–7.46 (m, 24H; ArH), 7.07 (brs, 4H; ArH), 7.02 (brs, 4H; ArH), 4.88 (d, J = 12.2 Hz, 2H; CH₂), 4.35 (d, J = 11.8 Hz, 2H; CH₂), 4.22–4.07 (m, 12H; OCH₂), 3.68 (d, $J_{\text{H-P}}$ = 14.0 Hz, 8H; CH₂), 3.60–3.51 (m, 4H; OCH₂), 3.09 (d, J = 11.5 Hz, 2H; CH₂), 3.01 (d, J = 11.8 Hz, 2H; CH₂); MS (FD): m/z (%): 1593.6 (23) [M] $^+$.

Tetrabromoacetamino calixarene 7: An aqueous solution of K₂CO₃ (2M, 20 mL) was added to a solution of the tetraamino calixarene **4c** (0.4 g, 0.64 mmol) in a mixture of THF (5 mL) and ethylacetate (10 mL). Bromoacetylchloride (6 mL) was then added in three portions to the vigorously stirred mixture. The reaction mixture was stirred for 2 h at room temperature and ethylacetate (50 mL) was then added. The organic layer was separated, washed with water (3 × 50 mL), dried with Na₂SO₄ and evaporated in vacuo, to give a white solid (0.6 g, 86%). M.p. 249–251 °C (decomp); ^1H NMR (400 MHz, CDCl₃/[D₆]DMSO, 10:1): δ = 9.47 (s, 4H; NH), 7.05, 7.03 (2brs, each 4H; ArH), 4.79, 4.22 (2d, J = 12.0 Hz, each 2H; CH₂), 4.10–3.40 (m, 16H; OCH₂), 3.00, 2.95 (2d, J = 12.0 Hz, each 2H; CH₂); MS (FD): m/z (%): 1108.2 (100) [M] $^+$.

Tetraphosphinate 6b: PhP(OEt)₂ (10 mL) was added to a solution of the tetrabromoacetamide **7** (0.2 g, 0.18 mmol) in THF (10 mL) and the reaction mixture was stirred at 70 °C for 48 h under nitrogen. The solution was then

poured into hexane (100 mL), and the precipitate formed was filtered off and washed with hexane. Two precipitations from THF/hexane gave 0.15 g (58%) of analytically pure **6b** as a white solid. M.p. 157–162 °C; ¹H NMR (400 MHz, [D₆]DMSO): δ = 9.75–9.68 (m, 4H; NH), 7.85–7.42 (m, 20H; ArH), 7.10, 7.05, 7.00 (3brs, 8H; ArH (calix)), 4.91, 4.36 (2brd, *J* = 11.3 Hz, each 2H; CH₂), 4.25–4.08 (m, 12H; CH₂), 4.05–3.93 (m, 4H; CH₂), 3.92–3.81 (m, 4H), 3.63–3.53 (m, 4H), 3.26–3.16 (m, 8H; CH₂), 3.11, 3.04 (2brd, *J* = 11.3 Hz, 2H each, CH₂), 1.23–1.15 (m, 12H; CH₃); MS (FD): *m/z* (%): 1465.2 (18) [*M*]⁺.

Tetraphosphonate 6c: A solution of the tetrabromoacetamide **7** (0.2 g, 0.18 mmol) in P(OEt)₃ (10 mL) was stirred at 70 °C for 64 h under nitrogen and then poured into hexane (50 mL) with stirring. The white precipitate that formed was filtered off and washed with hexane. The crude product, which contained P(OEt)₃, was additionally purified by precipitation from a CH₂Cl₂ solution by hexane to give a white solid (0.16 g, 67%). M.p. 140–142 °C; ¹H NMR (200 MHz, [D₆]DMSO): δ = 9.76 (s, 4H; NH), 7.19, 7.15 (2d, *J* = 2.0 Hz, each 4H; ArH), 4.96, 4.42 (2d, *J* = 11.9 Hz, each 2H; CH₂), 4.30–3.86 (m, 28H; OCH₂), 3.72–3.50 (m, 4H; OCH₂), 3.16, 3.09 (2d, *J* = 13.2 Hz, each 2H), 2.98 (d, *J* = 21.4 Hz, 8H; CH₂), 1.20 (t, *J* = 7.0 Hz, 24H; CH₃); MS (FD): *m/z* (%): 1338.4 (17) [*M*]⁺, 1360.3 (100) [*M*+Na]⁺, 1376.3 (16) [*M*+K]⁺.

General procedure for the preparation of tetrabromoacetamino calixarenes 9: A solution of the tetraamino calixarene **8** (2 g) in ethyl acetate (100 mL) and an aqueous solution of K₂CO₃ (2 M, 100 mL) were vigorously stirred. Bromoacetylchloride (5–7 mL) was added in two portions to the emulsion. After 20 min at RT, the organic layer was separated, washed with water (4 × 200 mL), dried over MgSO₄ and evaporated in vacuo. The residue was dissolved in the minimum amount of THF and reprecipitated with hexane to give analytically pure tetrabromoacetamide **9** as a white solid, which in all cases decomposed upon heating in the range 180–190 °C. Solutions of the tetrabromoacetamides in pure [D₆]DMSO were unstable.

Compound 9a: Yield 68%; ¹H NMR (200 MHz, CDCl₃/[D₆]DMSO, 20:1): δ = 9.30 (s, 4H; NH), 6.86 (s, 8H; ArH), 4.27 (d, *J* = 13.2 Hz, 4H; CH₂), 3.87 (s, 8H), 3.81 (t, *J* = 7.2 Hz, 8H; CH₂), 3.13 (d, *J* = 13.3 Hz, 4H; CH₂), 1.91 (m, 8H; CH₂), 0.98 (t, *J* = 7.2 Hz, 12H; CH₃); ¹³C NMR (100 MHz, CDCl₃/[D₆]DMSO, 10:1): δ = 163.44, 152.50, 134.07, 131.34, 119.47, 75.94, 30.39, 29.21, 22.09, 9.35; MS (FD): *m/z* (%): 1136.6 (100) [*M*]⁺, 1160.5 [*M*+Na]⁺; elemental analysis calcd (%) for C₄₈H₅₆N₄O₈Br₄: C 50.72, H 4.97, N 4.93; found C 51.05, H 5.34, N 4.73.

Compound 9b: Yield 72%; ¹H NMR (400 MHz, CDCl₃/[D₆]DMSO, 20:1): δ = 9.29 (s, 4H; NH), 6.85 (s, 8H; ArH), 4.42 (d, *J* = 13.3 Hz, 4H; CH₂), 3.87 (s, 8H; CH₂), 3.84 (t, *J* = 8.1 Hz, 8H; CH₂), 3.15 (d, *J* = 13.3 Hz, 4H; CH₂), 1.87 (m, 8H; CH₂), 1.36 (m, 16H; CH₂), 0.94 (t, *J* = 6.9 Hz, 12H; CH₃); ¹³C NMR (100 MHz, CDCl₃/[D₆]DMSO, 10:1): δ = 163.9, 153.2, 134.6, 131.4, 120.2, 74.8, 30.8, 29.5, 29.2, 27.8, 22.7, 13.6; MS (FD): *m/z* (%): 1249.0 (100) [*M*]⁺; elemental analysis calcd (%) for C₅₆H₇₂N₄O₈Br₄: C 53.86, H 5.81, N 4.50; found C 53.38, H 5.81, N 4.24.

Compound 9c: Yield 70%; ¹H NMR (200 MHz, CDCl₃/[D₆]DMSO, 20:1): δ = 9.29 (s, 4H; NH), 6.85 (s, 8H; ArH), 4.41 (d, *J* = 13.3 Hz, 4H; CH₂), 3.87 (s, 8H; CH₂), 3.83 (t, *J* = 7.5 Hz, 8H; CH₂), 3.13 (d, *J* = 13.3 Hz, 4H; CH₂), 1.89 (m, 8H; CH₂), 1.30 (m, 56H; CH₂), 0.88 (t, *J* = 6.6 Hz, 12H; CH₃); MS (FD): *m/z* (%): 1529.9 [*M*]⁺; elemental analysis calcd (%) for C₇₀H₁₁₂N₄O₈Br₄: C 59.69, H 7.38, N 3.66; found C 59.70, H 7.42, N 3.65.

General procedure for the Arbuzov reaction of 9 with P(OEt)₃: The bromoacetamide **9** (1.0 g) was dissolved or suspended in P(OEt)₃ (20–25 mL) and the mixture was stirred for 2–3 days at 60 °C under an inert atmosphere. The reaction mixture was poured into hexane (100 mL) and the precipitate formed was filtered off. In order to remove traces of P(OEt)₃, the crude product was precipitated from CH₂Cl₂ by hexane.

Tetraphosphonate 10a: Yield 77%; m.p. 188–191 °C; ¹H NMR (200 MHz, CDCl₃): δ = 8.64 (s, 4H; NH), 6.63 (s, 8H; ArH), 4.34 (d, *J* = 13.4 Hz, 4H; CH₂), 4.13 (m, 16H; CH₂), 3.77 (t, *J* = 7.3 Hz, 8H), 3.05 (d, *J* = 13.4 Hz, 4H; CH₂), 3.00 (d, *J* = 21.2 Hz, 8H; CH₂), 1.84 (m, 8H), 1.34 (t, *J* = 7.1 Hz, 24H; CH₃), 0.93 (t, *J* = 7.4 Hz, 12H; CH₃); MS (FD): *m/z* (%): 1366.2 (100) [*M*]⁺; elemental analysis calcd (%) for C₆₄H₉₆N₄O₂₀P₄ · 3H₂O: C 54.16, H 7.24, N 3.95; found C 53.88, H 7.18, N 4.00.

Tetraphosphonate 10b: Yield 76%; m.p. 167–170 °C; ¹H NMR (200 MHz, CDCl₃): δ = 8.68 (s, 4H; NH), 6.65 (s, 8H; ArH), 4.36 (d, *J* = 13.4 Hz, 4H; CH₂), 4.14 (m, 16H; CH₂), 3.82 (t, *J* = 7.2 Hz, 8H; CH₂), 3.08 (d, *J* = 13.4 Hz, 4H; CH₂), 3.00 (d, *J* = 21.2 Hz, 8H; CH₂), 1.81 (m, 8H; CH₂),

1.20–1.47 (m, 28H), 0.93 (t, *J* = 6.3 Hz, 12H; CH₃); ¹³C NMR (50 MHz, CDCl₃): δ = 162.5, 153.7, 135.0, 131.3, 121.5, 75.1, 69.7, 36.2 (d, *J* = 130 Hz), 31.3, 29.9, 28.3, 22.6, 16.3, 14.0; MS (FD): *m/z* (%): 1518.3 (100) [*M*+K]⁺; elemental analysis calcd (%) for C₇₂H₁₁₂N₄O₂₀P₄ · 2H₂O: C 57.13, H 7.72, N 3.70; found C 57.20, H 7.63, N 3.77.

Tetraphosphonate 10c: Yield 75%; m.p. 122–125 °C; ¹H NMR (200 MHz, CDCl₃): δ = 8.68 (s, 4H; NH), 6.64 (s, 8H; ArH), 4.35 (d, *J* = 13.4 Hz, 4H; CH₂), 4.15 (m, 24H; CH₂), 3.05 (d, *J* = 13.4 Hz, 4H; CH₂), 3.00 (d, *J* = 21.2 Hz, 8H; CH₂), 1.84 (m, 8H; CH₂), 1.35 (m, 68H), 0.88 (t, *J* = 6.5 Hz, 12H; CH₃); MS (FD): *m/z* (%): 1760.3 (100) [*M*]⁺; elemental analysis calcd (%) for C₉₂H₁₄₄N₄O₂₀P₄ · 7H₂O: C 58.90, H 8.49, N 2.99; found C, 59.06, H 8.43, N 2.90.

General procedure for the Arbuzov reaction of 9 with PhP(OEt)₂: The tetraphosphonates **10d,e** were prepared by the reaction of the corresponding tetrabromoacetamide with PhP(OEt)₂ (1:15 molar ratio) in the same way as the tetraphosphonates **10a–c**.

Tetraphosphinate 10d: Yield 65%; m.p. 151–154 °C; ¹H NMR (400 MHz, CDCl₃): δ = 8.66 (s, 4H; NH), 7.30–7.88 (m, 20H; ArH), 6.61 and 6.68 (2s, 8H; ArH), 4.34 (d, *J* = 13.4 Hz, 4H; CH₂), 3.85–4.17 (m, 8H), 3.77 (t, *J* = 7.3 Hz, 8H), 3.23–2.98 (m, 12H), 1.84 (m, 8H; CH₂), 1.26 (t, *J* = 7.0 Hz, 12H), 0.92 (t, *J* = 7.6 Hz, 12H; CH₃); ¹³C NMR (50 MHz, CDCl₃): δ = 162.5, 153.91, 136.75, 132.91, 131.60, 131.31, 129.06, 128.80, 121.72, 76.76, 61.72, 39.70 (d, *J* = 89.0 Hz), 31.14, 23.10, 16.39, 10.26; MS (FD): *m/z* (%): 1494.2 (100) [*M*]⁺; elemental analysis calcd (%) for C₈₀H₉₆N₄O₁₆P₄ · 2H₂O: C 62.82, H 6.59, N 3.66; found C 62.66, H 6.81, N 3.74.

Tetraphosphinate 10e: Yield 67%; m.p. 135–139 °C; ¹H NMR (400 MHz, CDCl₃): δ = 8.64 (s, 4H; NH), 7.32–7.89 (m, 20H; ArH), 6.64 and 6.68 (2s, 8H; ArH), 4.34 (d, *J* = 13.4 Hz, 4H; CH₂), 3.90–4.17 (m, 8H), 3.82 (t, *J* = 7.3 Hz, 8H), 3.12 (m, 12H), 1.84 (m, 8H; CH₂), 1.29 (m, 28H), 0.92 (t, *J* = 6.6 Hz, 12H; CH₃); ¹³C NMR (50 MHz, CDCl₃): δ = 162.5, 154.0, 135.1, 132.9, 131.7, 131.2, 129.5, 128.8, 121.8, 75.1, 61.8, 39.5 (d, *J* = 89.0 Hz), 31.1, 29.7, 28.3, 22.8, 16.5, 14.0. MS (FD): *m/z* (%): 1607.1 (100) [*M*]⁺.

Tetraphosphinic acid 11a: Me₃SiBr (0.25 mL, 2.0 mmol) was added to a solution of the phosphinate **10e** (0.4 g, 0.25 mmol) in dry CH₂Cl₂ (15 mL) and the reaction mixture was stirred at RT for 24 h under nitrogen. The solvent was evaporated in vacuo, and the residue was dried in vacuo to remove traces of SiMe₃Br. The solid trimethylsilyl ester was dissolved in absolute MeOH (15 mL), and the solution was stirred at RT for 12 h. Evaporation of methanol gave quantitatively the tetraphosphinic acid as a white solid. M.p. 150 °C (decomp); ¹H NMR (200 MHz, CD₃OD): δ = 7.38–8.00 (m, 20H; ArH), 6.78 (s, 8H; ArH), 4.44 (d, *J* = 13.0 Hz, 4H; CH₂), 3.91 (t, *J* = 7.0 Hz, 8H; CH₂), 3.14 (m, 12H; CH₂), 1.98 (m, 8H; CH₂), 1.46 (m, 16H; CH₂), 1.01 (t, *J* = 6.4 Hz, 12H; CH₃); MS (FD): *m/z* (%): 1495.7 (100) [*M*]⁺.

Tetraphosphonic acid 11b: This compound was prepared in the same way as **11a** by reacting the tetraphosphonate **10b** (0.4 g, 0.27 mmol) with SiMe₃Br (0.5 g, 4 mmol) and methanol (15 mL). White solid; m.p. 150 °C (decomp); ¹H NMR (200 MHz, CD₃OD/[D₆]DMSO, 5:1): δ = 6.81 (s, 8H; ArH), 4.38 (d, *J* = 13.4 Hz, 4H; CH₂), 3.83 (t, *J* = 7.0 Hz, 8H; CH₂), 3.00 (d, *J* = 13.4 Hz, 4H; CH₂), 2.88 (d, *J* = 22.7 Hz, 8H; CH₂), 1.88 (m, 8H; CH₂), 1.38 (m, 16H; CH₂), 0.93 (t, *J* = 7.0 Hz, 12H; CH₃).

NMR spectroscopic studies: All NMR spectra were recorded on an Avance DRX400 Bruker spectrometer equipped with a temperature controller. The 1D spectra were obtained by using a 90° pulse (7.5–9 μs) with 8 or 16K points. The COSY 2D spectra were typically recorded with 1024 data points in *t*₂ and 512 data points in *t*₁ with a bandwidth of 3–25 kHz. A zero-degree-shifted sine-bell apodization function was applied in both dimensions prior to the Fourier transformation. The EXSY experiments were performed by using the phase-sensitive pulse sequence (90°–*t*₁–90°–*t*_m–90°–AQ) with 2048*t*₂ × 2048*t*₁. Both dimensions were apodized by a shifted sin bell without zero-filling. The mixing time *t*_m was 20 ms for the paramagnetic Yb³⁺ complexes. A 500 ms mixing time was used in the ROESY experiments with spin-locking and with a 1024 × 512 data set. Zero-filling was applied to obtain a 1024 × 1024 size. Exchange and nOe cross peaks were distinguished by their sign, which was identical to or opposite to the sign of the diagonal peaks, respectively. Longitudinal relaxation times were collected at 20 MHz on a Minispec 120 (Bruker) at 25 °C and nuclear magnetic relaxation dispersion curves were recorded at the University of Mons-Hainaut (Belgium) on a field-cycling relaxometer described elsewhere.^[32] The anhydrous lanthanide perchlorate salts were prepared as

reported previously and all chemicals were handled under argon in a Jacomex glove box (Livry-Gargan, France). CAUTION: lanthanide perchlorates are potentially explosive when brought into contact with organic materials. It is advisable to use only small amounts of metal salt at a time with proper care and in a glove box.

Crystal structure determination: Single crystals of about $0.3 \times 0.3 \times 0.5$ mm (**5a**) and $0.2 \times 0.3 \times 0.4$ mm (**5b**) suitable for X-ray analysis were mounted on glass rods of 0.1 mm. The crystal data and the most relevant experimental parameters used in the X-ray measurements and in the crystal structure analyses are reported in Table 4. For both compounds the intensities were calculated from profile analyses according to the Lehmann and Larsen method.^[33] During the data collections, one standard reflection for each compound, collected every 100 scans, showed no significant fluctuations. The intensities were corrected for Lorentz and polarisation effects. Absorption effects were corrected by using ABSORB^[34] (max. and min. transmission factors: 1.15, 0.87 and 1.12, 0.86 for **5a** and **5b**, respectively). The two structures were solved by direct methods with SIR92^[35] and then completed by Fourier ΔF map and refined by blocked full-matrix least-squares methods on F by using SHELX76.^[36] In compound **5a** two independent molecules linked by hydrogen bonds were found in the asymmetric unit. For both compounds, the parameters refined were: the overall scale factor, the atomic coordinates and anisotropic atomic displacements for all the non-hydrogen atoms. The hydrogen atoms were located in the final Fourier ΔF maps and included at the last stages of the refinements with isotropic atomic displacements. The atomic-scattering factors of the non-hydrogen atoms were taken from Cromer and Waber,^[37] the values of Δf and $\Delta f'$ were those of Cromer and Ibers.^[38] The geometrical calculations were obtained by PARST.^[39] All the calculations were carried out on the Gould Encore91 of the Centro di Studio per la Strutturistica Diffraattometrica di C.N.R., Parma. Crystallographic data (excluding structure factors) have been deposited with the Cambridge Crystallographic Data Centre as supplementary publication no. CCDC-111834 (**5a**) and CCDC-111833 (**5b**). Copies of the data can be obtained free of charge on application to the Director, CCDC, 12 Union Road, Cambridge CB2 1EZ, UK (fax: (+44)1223-336-033; deposit@chemcrs.cam.ac.uk).

Acknowledgements

This work was supported by the European Community (Contract F14WCT 960022). JFD and BL gratefully acknowledge the financial support of the FNRS and the IISN of Belgium.

- [1] For general reviews on calixarenes see: a) V. Böhmer, *Angew. Chem.* **1995**, *107*, 785–818; *Angew. Chem. Int. Ed. Engl.* **1995**, *34*, 713–745; b) C. D. Gutsche, *Calixarenes Revisited* (Ed.: J. F. Stoddart), RSC, Cambridge, **1998**.
- [2] See for example: A. Casnati, *Gazz. Chem. Ital.* **1997**, *127*, 637–649.
- [3] a) J. Scheerder, J. F. Engbersen, D. N. Reinhoudt, *Recl. Trav. Chim. Pays Bas* **1996**, *115*, 307–320; b) F. P. Schmidtchen, M. Berger, *Chem. Rev.* **1997**, *97*, 1609–1646.
- [4] J. Scheerder, J. P. M. van Duynhoven, J. F. Engbersen, D. N. Reinhoudt, *Angew. Chem.* **1996**, *108*, 1172–1175; *Angew. Chem. Int. Ed. Engl.* **1996**, *35*, 1090–1093.
- [5] F. Arnaud-Neu, E. M. Collins, M. Deasy, G. Ferguson, S. J. Harris, B. Kaitner, A. J. Lough, M. A. McKervey, E. Marques, B. L. Ruhl, M.-J. Schwing-Weill, E. Sewart, *J. Am. Chem. Soc.* **1989**, *111*, 8681–8691.
- [6] M. Ogata, K. Fujimoto, S. Shinaki, *J. Am. Chem. Soc.* **1994**, *116*, 4505–4506.
- [7] See for example: a) N. Sabbatini, M. Guardigli, A. Mecati, V. Balzani, R. Ungaro, E. Ghidini, A. Casnati, A. Pochini, *J. Chem. Soc. Chem. Commun.* **1990**, 878–879; b) D. M. Rudkevich, W. Verboom, E. B. van der Tol, C. J. van Staveren, F. M. Kaspersen, J. W. Verhoeven, D. N. Reinhoudt, *J. Chem. Soc. Perkin. Trans. 2* **1995**, 131–134.
- [8] X. Chen, M. Ji, D. R. Fisher, C. M. Wai, *Chem. Commun.* **1998**, 377–378.
- [9] G. Montavon, G. Duplatre, Z. Asfari, J. Vicens, *Solvent Extr. Ion Exch.* **1997**, *15*, 169–188.
- [10] F. Arnaud-Neu, V. Böhmer, J.-F. Dozol, C. Grüttner, R. A. Jakobi, D. Kraft, O. Mauprivez, H. Rouquette, M.-J. Schwing-Weill, N. Simon, W. Vogt, *J. Chem. Soc. Perkin. Trans. 2* **1996**, 1175–1182.
- [11] The same approach was later realized in the case of cavitands: H. Boerrigter, W. Verboom, D. N. Reinhoudt, *J. Org. Chem.* **1997**, *62*, 7148–7155.
- [12] CMPO is used for carbamoylmethylphosphineoxides or carbamoylmethylphosphoryl compounds in general as well as for (*N,N*-diisobutylcarbamoylmethyl)octylphenylphosphineoxide **3** in particular throughout this article.
- [13] E. P. Horwitz, D. G. Kalina, H. Diamond, D. G. Vandegrift, W. W. Schultz, *Solvent Extr. Ion Exch.* **1985**, *3*, 75–109.
- [14] L. Delmau, N. Simon, M.-J. Schwing-Weill, F. Arnaud-Neu, J.-F. Dozol, S. Eymard, B. Tournois, V. Böhmer, C. Grüttner, C. Musigmann, A. Tunayar, *Chem. Commun.* **1998**, 1627–1628.
- [15] S. Barbosa, A. Garcia Carrera, S. E. Matthews, F. Arnaud-Neu, V. Böhmer, J.-F. Dozol, H. Rouquette, M.-J. Schwing-Weill, *J. Chem. Soc. Perkin Trans. 2* **1999**, 719–723.
- [16] For tetraesters of type **1b** showing rigidity owing to an aliphatic chain connecting two opposite *p*-positions see: F. Arnaud-Neu, V. Böhmer, L. Guerra, M. A. McKervey, E. F. Paulus, A. Rodriguez, M.-J. Schwing-Weill, M. Tabatabai, W. Vogt, *J. Chem. Soc. Perkin Trans. 2* **1992**, 1595–1601.
- [17] S. E. Matthews, M. Saadioui, V. Böhmer, S. Barbosa, F. Arnaud-Neu, M.-J. Schwing-Weill, A. Garcia Carrera, J.-F. Dozol, *J. Prakt. Chem.* **1999**, *341*, 264–273.
- [18] a) A. Arduini, M. Fabbi, M. Mantovani, L. Mirone, A. Pochini, A. Secchi, R. Ungaro, *J. Org. Chem.* **1995**, *60*, 1454–1457; b) A. Arduini, W. M. McGregor, D. Paganuzzi, A. Pochini, A. Secchi, F. Uguzzoli, R. Ungaro, *J. Chem. Soc. Perkin. Trans. 2* **1996**, 839–846.
- [19] A. Arduini, L. Mirone, D. Paganuzzi, A. Pochini, A. Secchi, R. Ungaro, *Tetrahedron* **1996**, *52*, 6011–6018.
- [20] M. Conner, V. Janout, S. L. Regen, *J. Am. Chem. Soc.* **1991**, *113*, 9670–9671.
- [21] This type of hydrogen bonding was detected in the crystalline state for a calix[4]arene tetrapropyl ether bearing in 1,3-positions two CMPO functions: E. F. Paulus, A. Shivanyuk, V. Böhmer, unpublished results.
- [22] D. G. Kalina, E. P. Horwitz, L. Kaplan, A. C. Muscatello, *Sep. Sci. Technol.* **1981**, *16*, 403–416.
- [23] J. A. Peters, J. Huskens, D. J. Raber, *J. Prog. Nucl. Magn. Reson. Spectrosc.* **1996**, *28*, 283–350.
- [24] B. Lambert, V. Jacques, A. Shivanyuk, S. E. Matthews, A. Tunayar, M. Baaden, G. Wipff, V. Böhmer, J. F. Desreux, *Inorg. Chem.*, in press.
- [25] S. Aime, M. Botta, M. Fasano, E. Terreno, *Chem. Soc. Rev.* **1998**, *27*, 19–29.
- [26] H. Diamond, P. Thiyagarajan, E. P. Horwitz, *Solvent Extr. Ion Exch.* **1990**, *8*, 503–513.
- [27] S. Cherfa, Ph.D. Thesis, University of Paris Sud, **1998**.
- [28] I. Bertini, O. Galas, C. Luchinat, G. Parigi, *J. Magn. Reson.* **1995**, *113*, 151–158.
- [29] I. A. Veselov, V. G. Shtyrlin, A. V. Zakharov, *Koord. Khim.* **1989**, *15*, 567–571.
- [30] E. Toth, D. Pubanz, S. Vauthey, L. Helm, A. E. Merbach, *Chem. Eur. J.* **1996**, *2*, 1607–1615.
- [31] F. Sansone, S. Barbosa, A. Casnati, D. Sciotto, R. Ungaro, *Tetrahedron Lett.* **1999**, *40*, 4741–4744.
- [32] P. Van der Elst, F. Maton, S. Laurent, F. Seghi, F. Chapelle, R. N. Muller, *Magn. Reson. Chem.* **1997**, *38*, 604–614.
- [33] M. S. Lehmann, F. K. Larsen, *Acta Crystallogr. Sect. A* **1974**, *30*, 580–584.
- [34] F. Uguzzoli, *Comput. Chem.* **1987**, *11*, 109–120.
- [35] A. Altomare, M. C. Burla, M. Camalli, G. Cascarano, C. Giacovazzo, A. Guagliardi, G. Polidori, *J. Appl. Crystallogr.* **1994**, *27*, 435–436.
- [36] G. Sheldrick, *SHELX76, Program for Crystal Structure Determinations*, University of Cambridge, England, **1976**.
- [37] D. T. Cromer, J. J. Waber in *International Tables for X-Ray Crystallography, Vol. IV* (Eds.: J. A. Ibers, W. C. Hamilton), Kynoch, Birmingham (England), **1974**, Table 2.2.B..
- [38] D. T. Cromer, J. A. Ibers, in *International Tables for X-Ray Crystallography, Vol. IV* (Eds.: J. A. Ibers, W. C. Hamilton), Kynoch, Birmingham (England), **1974**, Table 2.3.1..
- [39] M. Nardelli, *Comput. Chem.* **1983**, *7*, 95–102.

Received: December 29, 1999 [F2216]